Chemical Science

ROYAL SOCIETY OF CHEMISTRY

EDGE ARTICLE

View Article Online
View Journal | View Issue

Cite this: *Chem. Sci.*, 2021, **12**, 4361

All publication charges for this article have been paid for by the Royal Society of Chemistry

Received 23rd December 2020
Accepted 1st February 2021

DOI: 10.1039/d0sc06988d

rsc.li/chemical-science

Pressure-driven, solvation-directed planar chirality switching of cyclophano-pillar[5]arenes (molecular universal joints)†

Jiabin Yao, [a] Hiroaki Mizuno,[b] Chao Xiao, [a] Wanhua Wu, [a] Yoshihisa Inoue, *[c] Cheng Yang *[a] and Gaku Fukuhara *[bd]

Planar chiral cyclophanopillar[5]arenes with a fused oligo(oxyethylene) or polymethylene subring (**MUJ**s), existing as an equilibrium mixture of subring-included (in) and -excluded (out) conformers, respond to hydrostatic pressure to exhibit dynamic chiroptical property changes, leading to an unprecedented pressure-driven chirality inversion and the largest ever-reported leap of anisotropy (*g*) factor for the **MUJ** with a dodecamethylene subring. The pressure susceptivity of **MUJ**s, assessed by the change in *g* per unit pressure, is a critical function of the size and nature of the subring incorporated and the solvent employed. Mechanistic elucidations reveal that the in–out equilibrium, as the origin of the **MUJ**'s chiroptical property changes, is on a delicate balance of the competitive inclusion of subrings *versus* solvent molecules as well as the solvation of the excluded subring. The present results further encourage our use of pressure as a unique tool for dynamically manipulating various supramolecular devices/machines.

Introduction

Stimulus-responsive artificial molecular machines attract much research interest because of their ability to alter the structure and function through the molecular-level motion triggered by external factors.[1–3] A wide range of external stimuli, such as light,[4–6] temperature,[7,8] redox,[9–13] pH,[14] and chemical additives,[15–19] have hitherto been exploited to achieve diverse stimulus-responsive supramolecular architectures and devices with the aid of deep insights into the kinetic and thermodynamic driving forces involved.

Hydrostatic pressure is another fundamental and ubiquitous stimulus that is orthogonal to the other stimuli yet substantially influences various biological, chemical, and physical phenomena.[20–24] Indeed, hydrostatic pressure is known to cause the conformational changes of biomacromolecules, such as DNA,[25] RNA,[26] and proteins,[27] and also affect the molecular recognition events.[28–32] We have revealed that pressure can manipulate the supramolecular complexation and chiral photoreaction behaviors.[24,33–37] Despite these intriguing findings, the pressure effects on artificial supramolecular devices and molecular machines still remain an unchartered realm.

As a relatively new class of synthetic macrocyclic hosts, pillar[*n*]arenes (P[*n*]s) have been the target of intensive studies in the past decade.[38–47] In particular, planar chirality is one of the most intriguing aspects of P[*n*] chemistry.[48–50] In a recent study, we synthesized a series of inherently chiral cyclophano-P[5] and -P[6] termed molecular universal joints (**MUJ**s) and established their absolute configurations by comparing the experimental *versus* theoretical CD spectra.[51–54] The P[5]-based **MUJ1**–**MUJ3** (Scheme 1, left) employed in the present study incorporate a tetra(oxyethylene)-, dodecamethylene-, and hexa(oxyethylene)-bridged 1,4-hydroquinone unit, respectively, as a fused subring. The subring

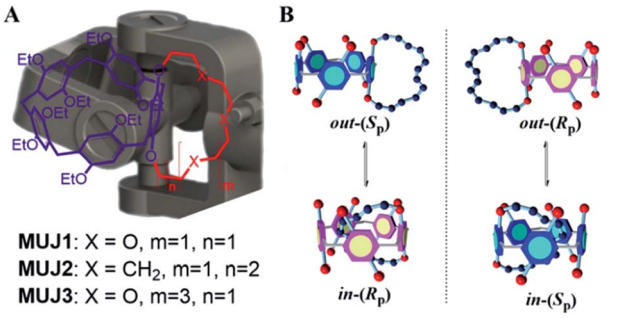

Scheme 1 Schematic illustration of chemical structures and chirality switching of **MUJ**s. (Left) Pillar[5]arene-based molecular universal joints (**MUJ**s). (Right) Schematic illustrations for the in–out equilibria of the enantiomeric pairs of **MUJ2**.

[a]*Key Laboratory of Green Chemistry & Technology of Ministry of Education, College of Chemistry, State Key Laboratory of Biotherapy, Healthy Food Evaluation Research Center, Sichuan University, Chengdu 610064, China. E-mail: yangchengyc@scu.edu.cn*

[b]*Department of Chemistry, Tokyo Institute of Technology, 2-12-1 Ookayama, Meguro-ku, Tokyo 152-8551, Japan. E-mail: gaku@chem.titech.ac.jp*

[c]*Department of Applied Chemistry, Osaka University, Suita 565-0871, Japan. E-mail: inoue@chem.eng.osaka-u.ac.jp*

[d]*JST, PRESTO, 4-1-8 Honcho, Kawaguchi, Saitama 332-0012, Japan*

† Electronic supplementary information (ESI) available. See DOI: 10.1039/d0sc06988d

introduced lowers the symmetry and makes the conformation before/after chiral inversion not enantiomeric anymore. As illustrated in Scheme 1 (right panel), the subring-included "in" and subring-excluded "out" conformers of the **MUJ** are interconvertible through tumbling of the 1,4-bridged hydroquinone unit, which however occurs only between the in-(R_p) and out-(S_p) and between the in-(S_p) and out-(R_p) isomers without any racemization.

We now report an unprecedented supramolecular chirality inversion of **MUJ**s, which is driven by hydrostatic pressure and facilitated or suppressed by solvation. We further elucidate its origin and operating mechanisms, the results of which allow us to develop a concept of using pressure as a powerful, otherwise-inaccessible, orthogonal-to-the-other-stimuli, yet widely applicable tool for manipulating supramolecular structures, properties, and functions and on/off-switching supramolecular devices and machines.

Results and discussion

Racemic **MUJ1–MUJ3** prepared as reported[51] were optically resolved by preparative chiral HPLC (Fig. S1–S3†). The second-eluted in-(R_p)/out-(S_p)-enantiomers of the **MUJ**s in 95–99% enantiomeric excess were used throughout the work. Using a high pressure vessel equipped with birefringence-free diamond windows for spectral measurements, we examined the effects of hydrostatic pressure on the UV-vis and circular dichroism (CD) spectra of in-(R_p)/out-(S_p)-**MUJ**s in hexane (*n*-H), methylcyclohexane (MCH), carbon tetrachloride (CTC), tetrahydrofuran (THF), ethyl acetate (EA), chloroform (CHL), dichloromethane (DCM), and acetonitrile (AN) at pressures from atmospheric 0.1 MPa to 320 or 160 (for CTC) MPa.

Fig. 1 shows the two extreme CD spectral behaviors observed for in-(R_p)/out-(S_p)-**MUJ2** in (a) AN and (b) EA upon gradual increase of pressure up to 320 MPa, while Fig. 2 summarizes the pressure-induced variation ranges of the anisotropy (g) factors of in-(R_p)/out-(S_p)-**MUJ1**, **MUJ2**, and **MUJ3** in all the examined solvents (see Fig. S4–S72 and Table S1† for the original data); note that $g = \Delta\varepsilon/\varepsilon$, where $\Delta\varepsilon$ denotes the molar CD and ε the molar extinction coefficient. By releasing the applied pressure, the original spectra were immediately recovered without any hysteresis, indicating that the pressure-induced changes observed are fully reversible and no chemical transformation or conformational lock is involved.

The g factor of in-(R_p)/out-(S_p)-**MUJ2** was a vital function of both pressure and solvent, exhibiting a dramatic sign-inversion in AN (Fig. 1a) in the middle of the applied pressure range, but no such behavior in EA (Fig. 1b). Thus, in AN, the g factors at 258 and 310 nm (g_{258} and g_{310}) are substantially enhanced (with a sign inversion) from −0.0035 to +0.0039 and from −0.0016 to +0.0034, respectively, by increasing the pressure from 0.1 to 320 MPa. The net change in g amounts to 0.0074 at 254 nm and to 0.0050 at 310 nm, which are the largest ever reported,[24,30] and are expected to grow further at yet higher pressures. In contrast, the g_{310} factor in EA merely shows a modest initial increase

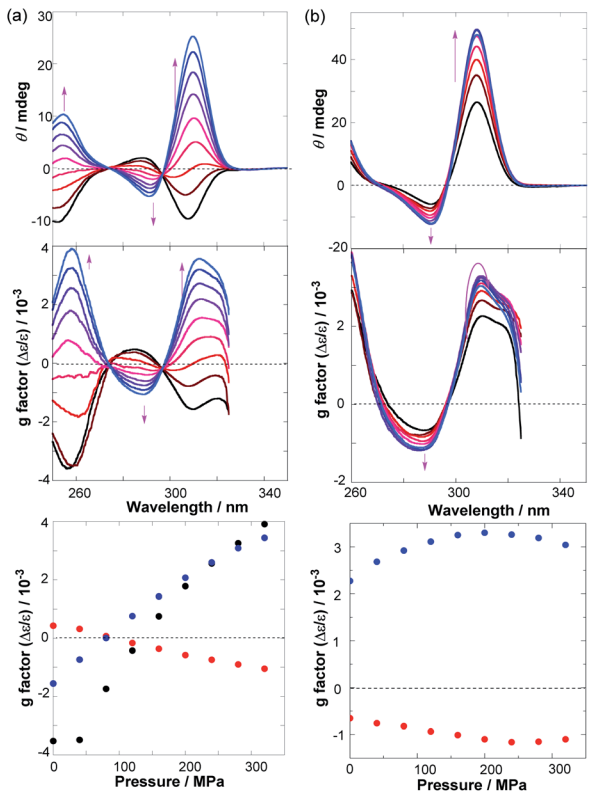

Fig. 1 Pressure-dependence of spectral analysis of in-(R_p)/out-(S_p)-**MUJ2**. (a) The CD (top) and anisotropy (g) factor (middle) spectra and the pressure-dependence of the g factors (bottom) monitored at 310 (blue), 288 (red), and 258 (black) nm for in-(R_p)/out-(S_p)-**MUJ2** (92 μM) in AN at room temperature. (b) The CD (top) and g factor (middle) spectra and the pressure-dependence of the g factors (bottom) at 309 (blue) and 288 (red) nm for in-(R_p)/out-(S_p)-**MUJ2** (136 μM) in EA at room temperature. Pressure applied: 0.1, 40, 80, 120, 160, 200, 240, 280, and 320 MPa (from black to light blue).

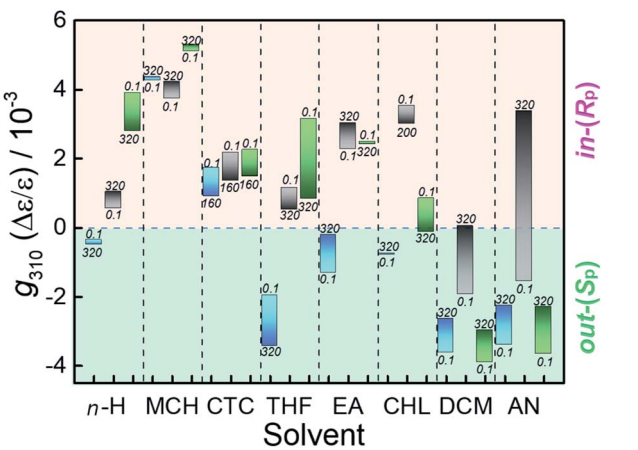

Fig. 2 Pressure effect for the g factor of **MUJ**s. Pressure-induced changes of the g factor at 310 (±1) nm (g_{310}) for in-(R_p)/out-(S_p)-**MUJ1** (blue), in-(R_p)/out-(S_p)-**MUJ2** (gray), and in-(R_p)/out-(S_p)-**MUJ3** (green) in hexane (*n*-H), methylcyclohexane (MCH), carbon tetrachloride (CTC), tetrahydrofuran (THF), ethyl acetate (EA), chloroform (CHL), dichloromethane (DCM), and acetonitrile (AN) at room temperature.

Table 1 Anisotropy factors at 310 (±1) nm under atmospheric pressure ($g_{310}{}^{0.1\ MPa}$) and overall pressure susceptivities of g_{310} ($\Delta g/\Delta P$) for **MUJ1–MUJ3** in various solvents

		$g_{310}{}^{0.1\ MPa}$ ($\times 10^3$)[b]			$\Delta g/\Delta P$[c] (TPa^{-1})		
Solvent	E_T[a]	**MUJ1**	**MUJ2**	**MUJ3**	**MUJ1**	**MUJ2**	**MUJ3**
n-H	30.9	−0.2	+0.6	+3.4	−0.7	+1.4	−2.6
MCH[d]	~31	+4.1	+3.7	+4.9	+0.6	+1.5	+0.9
CTC[d]	32.5	+1.7	+2.0	+2.2	−5.1[e]	−4.8[e]	−4.7[e]
THF[d]	37.4	−1.9	+1.2	+3.1	−4.9	−2.0	−7.1
EA	38.1	−1.2	+2.3	+2.4	+3.4	+2.4	−0.2
CHL[d]	39.1	−0.8	+3.4	+0.8	−0.0	−2.8[f]	−2.9
DCM	41.1	−3.6	−1.9	−3.9	+3.0	+5.9	+3.0
AN	46.0	−3.4	−1.6	−3.7	+3.5	+15.6	+4.2

[a] Reichardt's empirical solvent polarity parameter. [b] Positive (negative) $g_{310}{}^{0.1\ MPa}$ factor indicates preference for the in (out) conformer at atmospheric pressure. [c] $\Delta g/\Delta P = (g_{310}{}^{P_{max}} - g_{310}{}^{P_{min}})/(P_{max} - P_{min})$; the pressure range applied (ΔP): 0.1–320 MPa, unless noted otherwise. Positive (negative) $\Delta g/\Delta P$ value means equilibrium shift to the in-(R_p) (out-(S_p)) conformer upon pressurization. [d] Too bulky to be fully accommodated in the P[5] cavity (4.7 Å i.d.).[55–58] [e] ΔP: 0.1–160 MPa. [f] ΔP: 0.1–200 MPa.

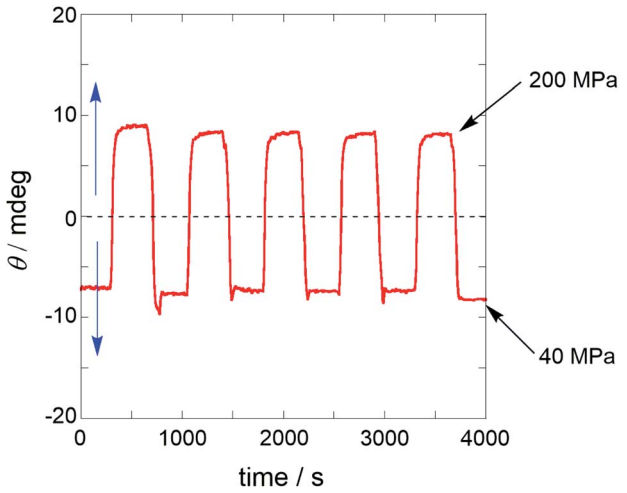

Fig. 3 Reversible switching of the ellipticity signal of in-(R_p)/out-(S_p)-**MUJ2** upon pressurization and depressurization. The ellipticity changes at 309 nm observed for an AN solution of in-(R_p)/out-(S_p)-**MUJ2** (92 μM) upon repeated pressurization–depressurization cycles between 40 and 200 MPa.

followed by a slow decrease to give a much smaller net change of 0.0007.

As can be seen from Fig. 2, the pressure-dependent CD spectral behaviors of the three **MUJ**s are distinctly different from each other in all the solvents examined (except CTC), but may be placed somewhere in between the two extreme cases mentioned above (Fig. 1a and b). One of the most intriguing (and unexpected) findings is the pressure-driven sign inversion of the *g* factor observed for **MUJ2** in DCM and AN. The same phenomenon is seen also for **MUJ3** in CHL and is anticipated to occur at much higher pressures for **MUJ1** in CTC, EA, DCM, and AN, for **MUJ2** in CTC, THF, and CHL, and for **MUJ3** in *n*-H, CTC, THF, DCM, and AN with a smaller pressure-dependence in most cases (Fig. 2).

In an attempt to elucidate the origin of the dynamic pressure-dependence (including the sign inversion) of the *g* factor observed for **MUJ2** in DCM and AN, we calculated the van der Waals volumes (V_{vdW}) of the out- and in-conformers of **MUJ**s geometry-optimized *in vacuo* by the DFT method at the B3LYP/6-31G(d) level. It turned out that the V_{vdW} obtained (Table S2†) is slightly larger for the out- than for the in-conformer, but the difference is mere 0.26–0.36 $Å^3$, which is rather negligible if compared with the whole volumes of the **MUJ**s (944–1030 $Å^3$). This result reveals that the difference in V_{vdW} between the naked in- and out-conformers is not a main driving force of the pressure-driven chirality switching of **MUJ**s.

Judging from the very disparate behaviors of *g* exhibited in different solvents (Fig. 2), we deduce that the pivotal role is played by solvent in determining the in/out conformation of **MUJ**s. Before closely examining the pressure effects, we analyze the original conformation of **MUJ2** at 0.1 MPa in all the solvents examined. Our recent study[51] has shown that the sign of the *g* factor is directly related to the in/out conformation of **MUJ2** and hence serves as a reliable tool for assessing the absolute configuration of the **MUJ**, *i.e.*, in-(R_p) or out-(S_p). This criterion and the *g* factor monitored at 310 nm under the atmospheric pressure ($g_{310}{}^{0.1\ MPa}$) listed in Table 1 indicate that, at 0.1 MPa, **MUJ2** favors the in-(R_p)-conformation in *n*-H, MCH, CTC, THF, EA, and CHL, but the out-(S_p)-conformation in DCM and AN.

To better understand the interaction of solvent molecules with the P[5] cavity, we attempted to determine the association constant (K_a) of the relevant solvents with 1,4-diethoxyP[5] (a model host with comparable cavity parameters) in MCH (a nonpolar/non-solvating molecule that is oversized and hence impenetrable into the P[5] cavity).[43] As shown in Table S3,† AN and DCM turned out to have 1–2 orders of magnitude higher affinities toward the P[5] cavity (K_a = 50–550 M^{-1}) than the other solvents (K_a = 4–18 M^{-1}), which well rationalizes the rich population of the out-(S_p) conformer in these two solvents at 0.1 MPa. In the other solvents of lower P[5] affinities, **MUJ2** includes the subring in its own cavity to form the in-(R_p) conformer and hence exhibits positive $g_{310}{}^{0.1\ MPa}$ factors at 0.1 MPa.

Possessing a polyether subring, **MUJ1** and **MUJ3** afford twice larger $g_{310}{}^{0.1\ MPa}$ factors of −3.4 to −3.9 × 10^{-3} than **MUJ2** in both DCM and AN (Table 1), indicating enriched populations of the out-(S_p)-conformers. This enrichment is most probably facilitated by the stabilization of the out-conformers through the solvation of the excluded polyether subring as well as the solvent inclusion in the P[5] cavity that is common to all the subring-excluded **MUJ**s. In less polar solvents of lower P[5] affinities, the g_{310} factor of **MUJ3**, though not exactly the same in magnitude, shares the same (positive) sign with that of **MUJ2**, while the g_{310} factor of **MUJ1** with the opposite sign behaves very differently in *n*-H, THF, EA, and CHL, implying nontrivial effects of the smaller subring on the in–out equilibrium. These observations and considerations led us to a tentative conclusion that the pressure-driven chirality inversion from out-(S_p)- to in-(R_p)-**MUJ2** observed in AN and DCM was caused by self-

inclusion of the dodecamethylene-subring accompanied by the exclusion of polar solvent molecule(s) originally residing in the P[5] cavity.

In order to substantiate the above hypothesis and quantitatively discuss the pressure effects on the in–out conformer equilibrium, we wanted to estimate the in/out ratio or the equilibrium constant ($K_{in/out}$ = [in]/[out]) from the observed g_{310} factor. This should be made possible if we could experimentally determine the g_{310} factors for both of the pure in-(R_p)- and out-(S_p)-**MUJ**s, or if we could determine one of them and could claim $g_{310}^{in} = -g_{310}^{out}$.

1,4-Dicyanobutane (DCB) is one of the strongest-binding guests for P[5] hosts,[59] and hence the addition of a large excess amount of DCB to an **MUJ** solution is expected to drive the subring out of the P[5] cavity. Upon addition of DCB of up to 2000 equivalents, the g_{310} factor gradually increased to reach a plateau in all the solvents. The ultimate values thus attained (Table S4†) are regarded as the g_{310} factors for pure out-(S_p)-conformers of **MUJ**s. However, these g_{310}^{out} factors for **MUJ1**–**MUJ3** are not close to each other, but depend on the subring incorporated in all the solvents used, thus being reduced by 20–30% on going from **MUJ3** to **MUJ1** and by 15–37% by increasing the solvent polarity (except CTC, which causes 46–47% reduction for unclear reasons; see Table S4†). These results imply that the g_{310}^{in} factors for pure in-(R_p)-**MUJ**s, if properly estimated, are also significantly affected by the internal and external factors, which means that postulating $g_{310}^{in} = -g_{310}^{out}$ is unrealistic.

Since experimentally determining the g_{310}^{in} factors for pure in-(R_p)-**MUJ**s was infeasible due to the lack of appropriate methods for completely driving the subring into the P[5] cavity, we semi-quantitatively discuss the pressure effects on the **MUJ** conformation. For this purpose, we simply define the overall pressure susceptivity of the chiroptical parameter g_{310} as $\Delta g/\Delta P = ({g_{310}}^{P_{max}} - {g_{310}}^{P_{min}})/(P_{max} - P_{min})$, despite that the pressure dependence is not necessarily homogeneous over the entire pressure range examined (Fig. S4–S72†).

The pressure susceptivities ($\Delta g/\Delta P$) thus evaluated for **MUJ2** (Table 1) are large positive (indicating a strong drive to the in-(R_p)-conformer upon pressurization) particularly in DCM and AN (amounting to +5.9 and +15.6 TPa^{-1}, respectively), but are much smaller positive or even negative, varying from +2.4 to −4.8 TPa^{-1}, in other solvents. We now comprehend why **MUJ2** achieves the pressure-induced chirality inversion in DCM and AN. Thus, the small negative initial ${g_{310}}^{0.1\ MPa}$ values (−1.9 and -1.6×10^{-3}) are readily cancelled out upon pressurization by the large positive $\Delta g/\Delta P$ values (+5.9 and +15.6 TPa^{-1}), eventually leading to a sign inversion within the pressure range employed. In contrast, the $\Delta g/\Delta P$ value has the same sign with ${g_{310}}^{0.1\ MPa}$ in *n*-H, MCH, and EA and no sign inversion is anticipated to occur upon pressurization, or is not sufficiently large to overwhelm the ${g_{310}}^{0.1\ MPa}$ factor even at the highest pressure applied in CTC and THF.

In polar DCM and AN, **MUJ1** and **MUJ3** less sensitively responded to pressure than **MUJ2** to give much smaller $\Delta g/\Delta P$ values of +3.0 to +4.2 TPa^{-1} (Table 1), for which the out-to-in equilibrium shift hindered by the solvation of the polyether subring that stabilizes the out-(S_p)-conformer should be responsible. Among the less polar solvents, CTC, THF, and CHL consistently afford negative $\Delta g/\Delta P$ values for all the **MUJ**s. Since the molar volume of the out-(S_p)-**MUJ**, particularly when solvated, is considered to be larger than that of the in-(R_p)-**MUJ**, the in-to-out equilibrium shift upon pressurization observed in CTC, THF, and CHL is unusual, indicating that the shift to the out-(S_p)-conformer under pressure is driven not by the volume difference but by other mechanisms.

CTC, THF, and CHL are too bulky to be fully accommodated in the P[5] cavity but could "perch" on the wide-opening ethoxy-decorated portal of the **MUJ**. Indeed, THF was found to be weakly bound to DEP[5] with $K_a = 4.12\ M^{-1}$ in MCH at 0.1 MPa by isothermal titration calorimetric (ITC) studies (Table S3†). Although the calorimetric titration at the same DEP[5] concentration (1 mM) did not produce any detectable heat upon addition of CHL or CTC, the NMR spectrum of DEP[5] (4–4.3 mM) in MCH-d_{14} showed small downfield shifts (0.10–0.13 ppm) of the aromatic and ethoxy protons in the presence of 2.8 M CHL (Fig. S79 and Table S5†); the least-square-means fit of the chemical shift changes to the 1 : 1 stoichiometry afforded $K_a = 0.63 \pm 0.02\ M^{-1}$ (Fig. S80†). In contrast, the addition of 5.18 M CTC caused slight upfield shifts (0.005–0.045 ppm) of the same protons, which are substantially smaller in magnitude and opposite in direction when compared with those observed upon addition of CHL (Table S5†) and AN (Table S7†). We conclude therefore that the slight shifts observed upon addition of CTC are irrelevant to the complexation but caused by the change in medium polarity. This conclusion is compatible with the very resembling pressure dependence behaviors commonly observed for all the **MUJ**s examined (Fig. 2 and Table 1). These results reveal that DEP[5] weakly interacts with the seemingly oversized guests (THF and CHL, but not CTC), probably at its ethoxy-decorated portal. Combining this fact and the significant CD spectral changes of **MUJ**s observed upon addition of CHL at elevated pressures (Fig. 2 and S22, S25, and S28†), we deduce that the supramolecular interaction of **MUJ**s with the modestly oversized molecules through portal perching is promoted under pressure.

The wide dynamic range, quick and reversible response to pressure change, and dynamic sign inversion of the CD signal prompted us to scrutinize the capability of **MUJ2** as a supramolecular chiroptical switching device driven by pressure.[60–63] Thus, a dilute solution of **MUJ2** in AN was subjected to repeated pressurization–depressurization cycles between 40 and 200 MPa to afford the alternating positive and negative ellipticities of comparable intensities with good reproducibility, as shown in Fig. 3.

Conclusions

In this study to elucidate the pressure dependence behaviors of conformationally flexible planar chiral cyclophano-pillar[5]arenes (**MUJ**s), we have shown that the in–out conformer equilibrium of **MUJ**s is highly susceptive to hydrostatic pressure particularly in polar solvents that possess strong affinities to the pillar[5]arene cavity to achieve the pressure-driven chirality switching and the largest ever reported jump of anisotropy

factor. These unique features of **MUJ**s open a new avenue for the multidimensional control of molecular machines and advanced piezo-sensitive materials by using pressure, temperature, and solvents, and also help us understand and utilize the pressure effects on natural and artificial supramolecular systems.[64–66]

Author contributions

G. F., C. Y. and Y. I. initiated the project. J. Y., H. M., C. X. and W. W. conceived and designed the experiments, analysed the data and prepared the manuscript, with input from all the authors. J. Y. conducted the chemical synthesis. G. F. and H. M. performed CD and UV-vis spectral analysis.

Conflicts of interest

There are no conflicts to declare.

Acknowledgements

We acknowledge the support of this work by the National Natural Science Foundation of China (No. 92056116, 21871194, 21572142), National Key Research and Development Program of China (No. 2017YFA0505903), Key R & D project of Science & Technology Department of Sichuan Province (2019YJ0160, 2019YJ0090, and 2017SZ0021), and State Key Laboratory of Fine Chemicals (KF 1508), Comprehensive Training Platform of Specialized Laboratory, College of Chemistry and Prof. Peng Wu of Analytical & Testing Center, Sichuan University. G. F. appreciates the generous supports by Grant-in-Aid for Scientific Research (B) (No. 19H02746) from the Japan Society for the Promotion of Science (JSPS) and Japan Science and Technology Agency (JST), PRESTO (No. JPMJPR17PA).

References

1 A. Coskun, M. Banaszak, R. D. Astumian, J. F. Stoddart and B. A. Grzybowski, *Chem. Soc. Rev.*, 2012, **41**, 19–30.
2 S. Kassem, A. T. L. Lee, D. A. Leigh, V. Marcos, L. I. Palmer and S. Pisano, *Nature*, 2017, **549**, 374–378.
3 K. Zhu, G. Baggi and S. J. Loeb, *Nat. Chem.*, 2018, **10**, 625–630.
4 J. J. D. de Jong, L. N. Lucas, R. M. Kellogg, J. H. van Esch and B. L. Feringa, *Science*, 2004, **304**, 278–281.
5 Z. Zheng, Y. Li, H. K. Bisoyi, L. Wang, T. J. Bunning and Q. Li, *Nature*, 2016, **531**, 352–356.
6 M. D. Poli, W. Zawodny, O. Quinonero, M. Lorch, S. J. Webb and J. Clayden, *Science*, 2016, **352**, 575–580.
7 M. Fujiki, *J. Am. Chem. Soc.*, 2000, **122**, 3336–3343.
8 T. Ooi, *Science*, 2011, **331**, 1395–1396.
9 S. Zahn and J. W. Canary, *Science*, 2000, **288**, 1404–1407.
10 H. Goto and E. Yashima, *J. Am. Chem. Soc.*, 2002, **124**, 7943–7949.
11 J. W. Canary, *Chem. Soc. Rev.*, 2009, **38**, 747–756.
12 E. Ohta, H. Sato, S. Ando, A. Kosaka, T. Fukushima, D. Hashizume, M. Yamasaki, K. Hasegawa, A. Muraoka, H. Ushiyama, K. Yamashita and T. Aida, *Nat. Chem.*, 2011, **3**, 68–73.
13 Y. J. Zhang, T. Oka, R. Suzuki, J. T. Ye and Y. Iwasa, *Science*, 2014, **344**, 725–728.
14 H. Liang, B. Hua, F. Xu, L.-S. Gan, L. Shao and F. Huang, *J. Am. Chem. Soc.*, 2020, **142**, 19772–19778.
15 V. V. Borovkov, T. Harada, Y. Inoue and R. Kuroda, *Angew. Chem., Int. Ed.*, 2002, **41**, 1378–1381.
16 Y. Qiu, P. Chen, P. Guo, Y. Li and M. Liu, *Adv. Mater.*, 2008, **20**, 2908–2913.
17 G. Haberhauer, *Angew. Chem., Int. Ed.*, 2010, **49**, 9286–9289.
18 E. Lee, H. Ju, I.-H. Park, J. H. Jung, M. Ikeda, S. Kuwahara, Y. Habata and S. S. Lee, *J. Am. Chem. Soc.*, 2018, **140**, 9669–9677.
19 Y.-F. Yang, W.-B. Hu, L. Shi, S.-G. Li, X.-L. Zhao, Y. A. Liu, J.-S. Li, B. Jiang and W. Ke, *Org. Biomol. Chem.*, 2018, **16**, 2028–2032.
20 F. Zhao, Y. Zhao, H. Cheng and L. Qu, *Angew. Chem., Int. Ed.*, 2015, **54**, 14951–14955.
21 Y. Zhang, J. Yu, H. N. Bomba, Y. Zhu and Z. Gu, *Chem. Rev.*, 2016, **116**, 12536–12563.
22 Y. Ishijima, H. Imai and Y. Oaki, *Chem*, 2017, **3**, 509–521.
23 Y. Sagara, N. Tamaoki and G. Fukuhara, *ChemPhotoChem*, 2018, **2**, 959–963.
24 T. Kosaka, S. Iwai, G. Fukuhara, Y. Imai and T. Mori, *Chem.–Eur. J.*, 2019, **25**, 2011–2018.
25 S. Takahashi and N. Sugimoto, *Angew. Chem., Int. Ed.*, 2013, **52**, 13774–13778.
26 A. Krzyżaniak, J. Barciszewski, J. P. Fürste, R. Bald, V. A. Erdmann, P. Salański and J. Jurczak, *Int. J. Biol. Macromol.*, 1994, **16**, 159–162.
27 K. Heremans and L. Smeller, *Biochim. Biophys. Acta, Protein Struct. Mol. Enzymol.*, 1998, **1386**, 353–370.
28 K. Ariga, Y. Terasaka, D. Sakai, H. Tsuji and J. Kikuchi, *J. Am. Chem. Soc.*, 2000, **122**, 7835–7836.
29 B. Neumann and P. Pollmann, *Phys. Chem. Chem. Phys.*, 2000, **2**, 4784–4792.
30 Y. Nagata, R. Takeda and M. Suginome, *Chem. Commun.*, 2015, **51**, 11182–11185.
31 Y. Wang, X. Tan, Y.-M. Zhang, S. Zhu, I. Zhang, B. Yu, K. Wang, B. Yang, M. Li, B. Zou and S. X.-A. Zhang, *J. Am. Chem. Soc.*, 2015, **137**, 931–939.
32 C. Liu, G. Xiao, M. Yang, B. Zou, Z.-L. Zhang and D.-W. Pang, *Angew. Chem., Int. Ed.*, 2018, **57**, 1893–1897.
33 Y. Inoue, E. Matsushima and T. Wada, *J. Am. Chem. Soc.*, 1998, **120**, 10687–10696.
34 M. Kaneda, S. Asaoka, H. Ikeda, T. Mori, T. Wada and Y. Inoue, *Chem. Commun.*, 2002, 1272–1273.
35 C. Yang, A. Nakamura, G. Fukuhara, Y. Origane, T. Mori, T. Wada and Y. Inoue, *J. Org. Chem.*, 2006, **71**, 3126–3136.
36 C. Yang, T. Mori, Y. Origane, Y. H. Ko, N. Selvapalam, K. Kim and Y. Inoue, *J. Am. Chem. Soc.*, 2008, **130**, 8574–8575.
37 M. Gao, W. Zhang and L. Zhang, *Nano Lett.*, 2018, **18**, 4424–4430.
38 T. Ogoshi, S. Kanai, S. Fujinami, T. Yamagishi and Y. Nakamoto, *J. Am. Chem. Soc.*, 2008, **130**, 5022–5023.

39 D. Cao, Y. Kou, J. Liang, Z. Chen, L. Wang and H. Meier, *Angew. Chem., Int. Ed.*, 2009, **48**, 9721–9723.
40 Y. Ma, Z. Zhang, X. Ji, C. Han, J. He, Z. Abliz, W. Chen and F. Huang, *Eur. J. Org. Chem.*, 2011, **2011**, 5331–5335.
41 X.-B. Hu, Z. Chen, L. Chen, L. Zhang, J.-L. Hou and Z.-T. Li, *Chem. Commun.*, 2012, **48**, 10999–11001.
42 T. Ogoshi, T. Yamagishi and Y. Nakamoto, *Chem. Rev.*, 2016, **116**, 7937–8002.
43 K. Jie, Y. Zhou, E. Li, R. Zhao and F. Huang, *Angew. Chem., Int. Ed.*, 2018, **57**, 12845–12849.
44 H. Zhang, Z. Liu and Y. Zhao, *Chem. Soc. Rev.*, 2018, **47**, 5491–5528.
45 E. Li, Y. Zhou, R. Zhao, K. Jie and F. Huang, *Angew. Chem., Int. Ed.*, 2019, **58**, 3981–3985.
46 P. Xin, H. Kong, Y. Sun, L. Zhao, H. Fang, H. Zhu, T. Jiang, J. Guo, Q. Zhang, W. Dong and C.-P. Chen, *Angew. Chem., Int. Ed.*, 2019, **58**, 2779–2784.
47 W. Yang, K. Samanta, X. Wan, T. U. Thikekar, Y. Chao, S. Li, K. Du, J. Xu, Y. Gao, H. Zuilhof and A. C.-H. Sue, *Angew. Chem., Int. Ed.*, 2020, **59**, 3994–3999.
48 T. Ogoshi, K. Masaki, R. Shiga, K. Kitajima and T. Yamagishi, *Org. Lett.*, 2011, **13**, 1264–1266.
49 T. Ogoshi, T. Akutsu, D. Yamafuji, T. Aoki and T. Yamagishi, *Angew. Chem., Int. Ed.*, 2013, **52**, 8111–8115.
50 S.-H. Li, H.-Y. Zhang, X. Xu and Y. Liu, *Nat. Commun.*, 2015, **6**, 7590.
51 J. Yao, W. Wu, W. Liang, Y. Feng, D. Zhou, J. J. Chruma, G. Fukuhara, T. Mori, Y. Inoue and C. Yang, *Angew. Chem., Int. Ed.*, 2017, **56**, 6869–6873.
52 C. Fan, J. Yao, G. Li, C. Guo, W. Wu, D. Su, Z. Zhong, D. Zhou, Y. Wang, J. J. Chruma and C. Yang, *Chem.–Eur. J.*, 2019, **25**, 12526–12537.
53 J. Ji, Y. Li, C. Xiao, G. Cheng, K. Luo, Q. Gong, D. Zhou, J. J. Chruma, W. Wu and C. Yang, *Chem. Commun.*, 2020, **56**, 161–164.
54 C. Xiao, W. Wu, W. Liang, D. Zhou, K. Kanagaraj, G. Cheng, D. Su, Z. Zhong, J. J. Chruma and C. Yang, *Angew. Chem., Int. Ed.*, 2020, **59**, 8094–8098.
55 F. Guo, Y. Sun, B. Xi and G. Diao, *Supramol. Chem.*, 2018, **30**, 81–92.
56 K. Jie, Y. Zhou, E. Li and F. Huang, *Acc. Chem. Res.*, 2018, **51**, 2064–2072.
57 M. Panneerselvam, M. D. Kumar, M. Jaccob and R. V. Solomon, *ChemistrySelect*, 2018, **3**, 1321–1334.
58 C. Schönbeck, H. Li, B.-H. Han and B. W. Laursen, *J. Phys. Chem. B*, 2015, **119**, 6711–6720.
59 Y. Wang, G. Ping and C. Li, *Chem. Commun.*, 2016, **52**, 9858–9872.
60 D. Fichou, C. Hubert and F. Garnier, *Adv. Mater.*, 1995, **7**, 914–917.
61 B. Onida, L. Borello, S. Fiorilli, B. Bonelli, C. O. Areán and E. Garrone, *Chem. Commun.*, 2004, 2496–2497.
62 T. Kosaka, Y. Inoue and T. Mori, *J. Phys. Chem. Lett.*, 2016, **7**, 783–788.
63 T. Kosaka, S. Iwai, Y. Inoue, T. Moriuchi and T. Mori, *J. Phys. Chem. A*, 2018, **122**, 7455–7463.
64 D. Bartlett, M. Wright, A. A. Yayanos and M. Silverman, *Nature*, 1989, **342**, 572–574.
65 B. Fromy, E. Lingueglia, D. Sigaudo-Roussel, J. L. Saumet and M. Lazdunski, *Nat. Med.*, 2012, **18**, 1205–1207.
66 W.-Z. Zeng, K. L. Marshall, S. Min, I. Daou, M. W. Chapleau, F. M. Abboud, S. D. Liberles and A. Patapoutian, *Science*, 2018, **362**, 464–467.